Available online at www.sciencedirect.com

ScienceDirect

journal homepage: www.keaipublishing.com/en/journals/geog;
http://www.jgg09.com/jweb_ddcl_en/EN/volumn/home.shtml

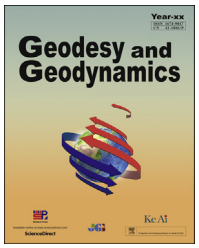

Characteristics of regional crustal deformation before 2016 Menyuan Ms6.4 earthquake

Weitao Chen[a], *Weijun Gan*[b,*], *Genru Xiao*[c], *Yuebing Wang*[a], *Weiping Lian*[a], *Shiming Liang*[b], *Keliang Zhang*[b]

[a] *National Earthquake Infrastructure Service, China Earthquake Administration, Beijing 100036, China*
[b] *State Key Laboratory of Earthquake Dynamics, Institute of Geology, China Earthquake Administration, Beijing 100029, China*
[c] *Faculty of Geomatics, East China University of Technology, Fuzhou 344000, China*

ARTICLE INFO

Article history:
Received 21 March 2016
Accepted 14 May 2016
Available online 29 July 2016

Keywords:
2016 Menyuan Ms6.4 earthquake
GPS observation
Crustal deformation
Seismic moment accumulation rate
Dilatation
Maximum shear strain

ABSTRACT

On January 21, 2016, a strong earthquake with a magnitude of Ms6.4 happened at Menyuan, Qinghai Province of China. In almost the same place, there was another strong earthquake happened in 1986, with similar magnitude and focal mechanism. In this paper, we analyze the characteristics of regional crustal deformation before the 2016 Menyuan Ms6.4 earthquake by using the data from 10 continuous Global Positioning System (GPS) stations and 74 campaign-mode GPS stations within 200 km of this event: (a) Based on the velocity field from over ten years GPS observations, a regional strain rate field is calculated. The results indicate that the crustal strain rate and seismic moment accumulation rate of the Qilian-Haiyuan active fault, which is the seismogenic tectonics of the event, are significantly higher than the surrounding regions. In a 20 km × 20 km area around the seismogenic region, the maximum and minimum principal strain rates are 21.5 nanostrain/a (NW–SE extension) and −46.6 nanostrain/a (NE–SW compression), respectively, and the seismic moment accumulation rates is 17.4 Nm/a. The direction of principal compression is consistent with the focal mechanism of this event. (b) Based on the position time series of the continuous GPS stations for a time-span of about 6 years before the event, we calculate the strain time series. The results show that the dilatation of the seismogenic region is continuously reduced with a "non-linear" trend since 2010, which means the seismogenic region has been in a state of compression. However, about 2–3 months before the event, both the dilatation and maximum shear strain show significant inverse trends. These

* *Corresponding author.*
E-mail address: wjgan@gps.gov.cn (W. Gan).
Peer review under responsibility of Institute of Seismology, China Earthquake Administration.

Production and Hosting by Elsevier on behalf of KeAi

http://dx.doi.org/10.1016/j.geog.2016.07.003

abnormal changes of crustal deformation may reflect the non-linear adjustment of the stress–strain accumulation of the seismogenic region, when the accumulation is approaching the critical value of rupture.

How to cite this article: Chen W, et al., Characteristics of regional crustal deformation before 2016 Menyuan *Ms*6.4 earthquake, Geodesy and Geodynamics (2016), 7, 275–283, http://dx.doi.org/10.1016/j.geog.2016.07.003.

1. Introduction

On January 21, 2016, a strong earthquake with a magnitude of Ms6.4 happened at Menyuan, Qinghai Province of China. The epicenter is N37.68°, E101.62°, and the focal depth is about 10 km. The result of seismic moment tensor shows this event is thrust and strike-slip. The fault plane I has a strike of 335°, a dip of 53° and a rake of 98°, and the fault plane II has a strike of 141°, a dip of 38° and a rake of 79°. The epicenter is located adjacent to the Lenglongling Fault, which is a Holocene active fault with left-lateral and thrust slip, striking of NW (http://www.eq-igl.ac.cn/upload/images/2016/1/2191153838.jpg). Notice that in almost the same place, there was another strong earthquake happened in 1986 [1]. The USGS CMT shows that the parameters of the two fault planes of the earthquake are (strike 125°, dip 37°, rake 55°) and (strike 346°, dip 60°, rake 113°), respectively, which are similar to the 2016 event. (http://earthquake.usgs.gov/earthquakes/eventpage/usp0002xjb#moment-tensor?source=us&code=gcmt19860826094304). As the recurrence of these two Ms6.4 earthquakes in the same place may have the implication of "characteristic earthquake", we try to analyze the characteristic of regional crustal deformation before 2016 Menyuan Ms6.4 earthquake so as to find some precursors for the predication of the next characteristic earthquake in this area.

2. GPS data and data processing

In the northeastern margin of the Tibetan Plateau, two national scientific infrastructure projects named "Crustal Movement Observation Network of China" (CMONOC I) and "Tectonic and Environmental Observation Network of Mainland China" (CMONOC II) have deployed dense GPS stations, and accumulated high-quality GPS observation data since 1999 [2,3] (Fig. 1). Here we chose the data from 10 continuous GPS stations and 74 campaign-mode GPS stations within 200 km of the seismogenic region. The more detailed information about the GPS stations is listed in Table 1.

GPS data were processed with the software GIPSY/OASIS (Version 6.0) [4] from Jet Propulsion Laboratory (JPL), National Aeronautics and Space Administration (NASA), using the Precise Point Positioning (PPP) strategy and JPL products to obtain daily loosely constrained solutions. Then, we use the software QOCA of JPL [5], to perform joint adjustment for the daily loosely constrained solutions of all stations to get their coordinate time series and optimum estimations of velocity in the International Terrestrial Reference Frame (ITRF) 2008. The specific procedures are described below:

The linear combinations reducing or eliminating the effect of ionospheric delay are taken as observational variables. The satellite truncation altitude angle is 15°, and data sampling rate is 300 s. Fixed International GNSS Service (IGS) 08-based precise obits and clocks of JPL are adopted (http://sideshow.jp1.nasa.gov). The a priori global pressure and temperature model (GPT) and global-mapping function (GMF) are used [6]. Correction for ocean tide loading is made with the Finite Element Solution (FES) 2004 model with online calculation (http://holt.oso.chalmers.se/loading). During data processing, the self-consistency of the products are taken into consideration, such as the orbits, clock difference, satellite-dependent differential code biases (DCB), phase center of receiver antenna and phase center of satellite [7]. The estimation parameters include station coordinates, clock errors of receivers and troposphere delay. To improve solution accuracy, we apply the Ambizap software [8] for phase ambiguity resolving, in which various linear combinations of observational parameters are determined using the fixed point theorems, and the unique and self-consistent daily solutions with phase ambiguity resolved are generated in the end. Finally, through seven parameter transform, the daily solutions are converted into ITRF2008 reference system.

3. Interseismic GPS velocity field

Fig. 2 shows the GPS velocity field in a Eurasia-fixed reference frame, which clearly demonstrates that the velocities on the south side of the Qilian-Haiyuan fault system, the seismogenic tectonic of 2016 Menyuan Ms6.4 earthquake, are generally larger than those on the north side. The average crustal motion rate is 9.5 mm/a for the 45 stations in the south and 4.0 mm/a for the 39 stations in the north, which indicates a difference of 5.5 mm/a. That is, the Qilian-Haiyuan fault system accommodates a remarkable part of the NEE extrusion in this region.

In order to determine the slip rate of Qilian-Haiyuan fault system by GPS velocity field, especially for the left-lateral

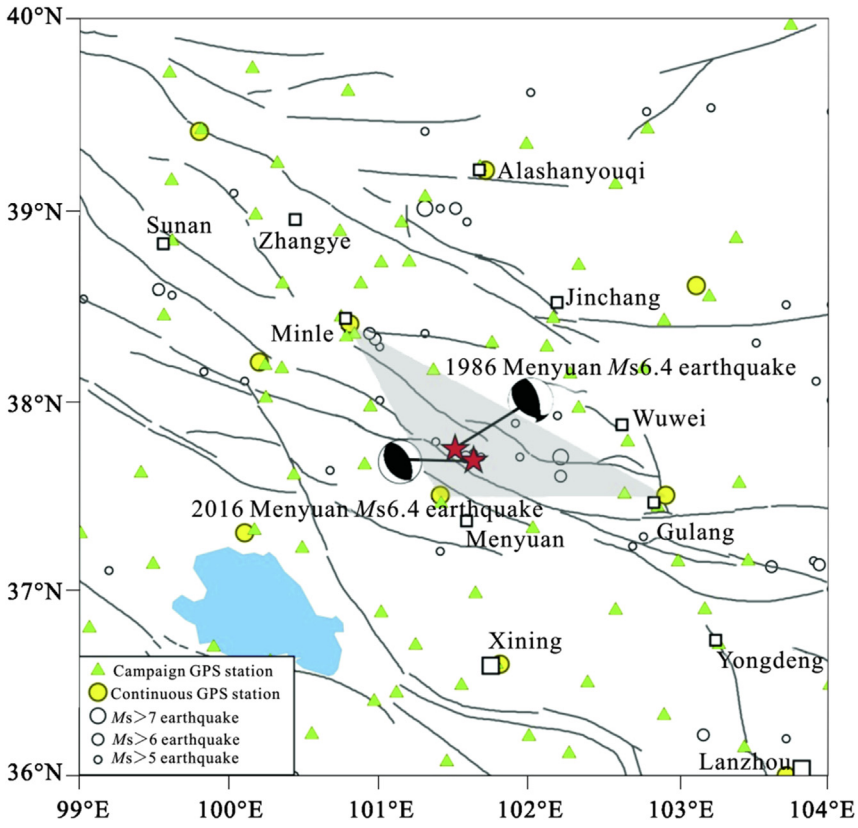

Fig. 1 – Active faults and GPS stations around 2016 Menyuan Ms6.4 earthquake. The yellow circles indicate continuous GPS station, and the green triangles denote campaign-mode GPS station. The shadow triangle region covering the earthquakes is formed by 3 continuous GPS stations.

and dip-slip rates of Lenglongling Fault, the most possible seismogenic fault of 2016 Menyuan Ms6.4 earthquake, we first construct a simple geometric model for the major active faults based on the Yuan's geology result (Fig. 3) [9]. The fault parameters, such as dip direction, dip angle, and locking depths, are shown in Table 2. Then, we inversed the slip rates of these faults based on the elastic half-space dislocation model [10] constrained by GPS velocities. The results indicate that the left-lateral slip rate and thrust rate of the Lenglongling Fault are 4.6 ± 0.8 mm/a and 5.9 ± 0.8 mm/a, respectively [Table 2], which means that there is a significant strain energy accumulation rate on this seismogenic fault.

4. Interseismic strain rate field

Considering that the characteristics of a GPS velocity field are definitely related to the selection of a reference frame, we use GPS velocity field to calculate the crustal strain rate field, which is independent from a reference frame; and then to analyze the crustal deformation characteristics of the seismogenic region with strain rate field.

Table 1 – The information of GPS stations used in this study.

GPS stations	Type of operation	Observation	Project
G153,G158,G152,G148,G133,G143,G146,G140,G157,G044, G075,G062,G090,G048,G054,G071,G076,G097,G051,G045, G059,G065,G094,G082,G100,G141,G084,G055,G070,G103, G089,G080,G047,G058,G096,G074,G060,G057,G098,G061, G064,G134,G087,G081,G049,G066,G063,G046,G069,G056, G093,G073,G079,G053,G083,G050,G068,G095,G091,G092	Campaign-mode	Sampling rate: 30 s, observed in 1999, 2001, 2004, 2007, 2009, 2011, 2013 and 2015 with an occupation of at least 3 days for each station	CMONOC I
G306,G307,G318,G320,G321,G327,G329,G330,G331,G334, G336,G337,G338, G351	Campaign-mode	Sampling rate: 30 s, observed in 2009, 2011, 2013 and 2015 with an occupation of at least 3 days for each station	CMONOC II
XNIN,GSGL,GSGT,GSLZ,GSML,GSMQ,NMAY,QHGC, QHME,QHQL	Continuous	Sampling rate: 30 s, 2009–2016	CMONOC II

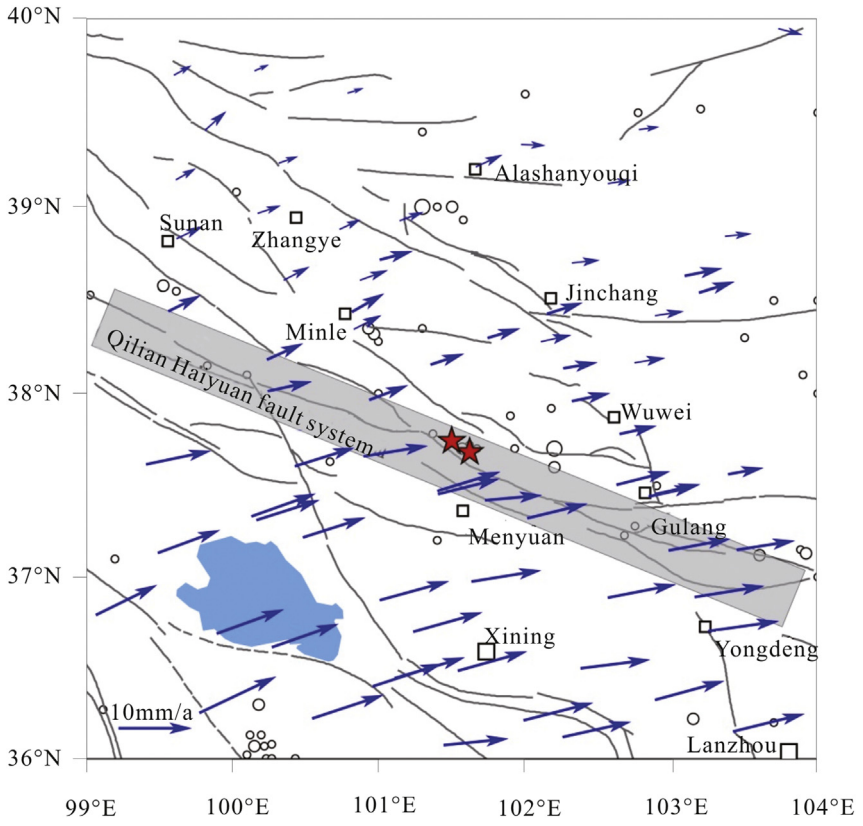

Fig. 2 – Horizontal GPS velocities around the epicenter of the 2016 Ms6.4 earthquake (relative to stable Eurasia). It can be seen that the GPS velocities are obviously different between the two sides of the Qilian-Haiyuan fault system.

4.1. *Regional crustal strain rate and seismic moment accumulation rate*

In order to get a continuous strain rate map of the region, we use a "spline in tension" technique [11,12] with the tension parameter $\tau = 0.95$ to interpolate the GPS velocities on a $0.1^\circ \times 0.1^\circ$(longitude and latitude) grids, and then calculate the strain rate tensor in every $0.2^\circ \times 0.2^\circ$ area with the nine interpolated velocities on the grids. This method produces a reliable strain result, especially for the area where the distribution of observed velocities is dense. Fig. 4 shows the strain rate field of this region. It can be seen that the strain accumulation rate along the Qilian-Haiyuan fault system is significant with $\dot{\varepsilon}_1 = 21.5$ nanostrain/a (NW–SE extension) and $\dot{\varepsilon}_2 = -46.6$ nanostrain/a (NE–SW compression) on average. The direction of principal compression strain rate is consistent with the focal mechanism of the 2016 and 1986 Menyuan *Ms*6.4 earthquakes. Therefore, the principal strain tensor obtained by GPS velocities could be used to determine the focal mechanism of strong earthquakes in a region.

Further, we could calculate the regional seismic moment accumulation rate by using the regional strain rate and simplified Kostrov formula [13]:

$$M_0 = 2\mu A H_s \mathrm{Max}(|\dot{\varepsilon}_1|, |\dot{\varepsilon}_2|, |\dot{\varepsilon}_1 + \dot{\varepsilon}_2|) \quad (1)$$

where M_0 is the rate of seismic moment accumulation, μ is the rigidity of the elastic layer, A is the area of concerned region, Hs is the seismogenic thickness over which elastic strain accumulates and is dissipated in earthquakes. $\mathrm{Max}(|\dot{\varepsilon}_1|, |\dot{\varepsilon}_2|, |\dot{\varepsilon}_1 + \dot{\varepsilon}_2|)$ is equal to the largest value of $|\dot{\varepsilon}_1|$, $|\dot{\varepsilon}_2|$ and $|\dot{\varepsilon}_1 + \dot{\varepsilon}_2|$, $\dot{\varepsilon}_1$ and $\dot{\varepsilon}_2$ are the principal surficial extension and contraction rates. H_s and μ are commonly assumed as approximately 15 km and 3×10^{10} Nm^{-2}, respectively, for the northeastern margin of the Tibetan Plateau. Thus, based on the smoothed strain rate field of $0.2^\circ \times 0.2^\circ$ grid (approximately 20 km × 20 km), we deduced the seismic moment accumulation rate map of this region (Fig. 5). The result shows there is an outstanding sub-region (approximately 20 km × 20 km) near the epicenter of the 2016 Menyuan Ms6.4 earthquake with value as large as 17.4 Nm/a on average, which is significantly higher than other section of Qilian-Haiyuan fault system.

4.2. *The characteristics of regional strain variation time series*

In order to analyze and determine the minor anomalies of crustal deformation before the earthquake, we calculate the dilatation and maximum shear strain time series in a triangle area (Fig. 1), which is formed by 3 continuous GPS stations (GSML, GSGL and QHME) and covering the seismogenic region of the 2016 Menyuan *Ms*6.4 earthquake. The results show the dilatation at seismogenic region is continuously reduced with a "non-linear" trend since 2010, which means the seismogenic region has been in a state of compression. However, about 2–3 months before the event, both the

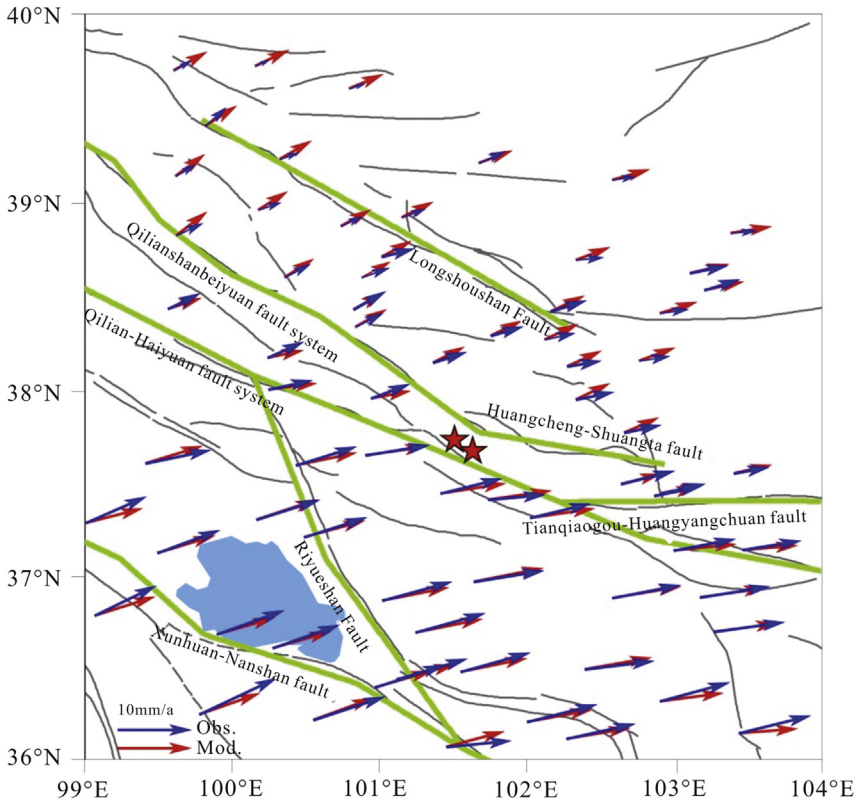

Fig. 3 – Geometric model of the major active faults and the GPS velocities around the seismogenic area of the 2016 Menyuan Ms6.4 earthquake. The grey thin lines indicate active faults, and the green thick lines, the modeled major active faults. The blue vectors indicate observed GPS velocities, and the red vectors arrows, calculated velocities using the elastic half-space dislocation mode.

dilatation and maximum shear strain show significant inverse trends (Fig. 6). These abnormal changes of crustal deformation may reflect the non-linear adjustment of the stress–strain accumulation of the seismogenic region, when the accumulation is approaching the critical value of rupture.

5. Discussion

For the above mentioned non-linear or abnormal changes of the dilatation and maximum shear strain, which are calculated by 3 continuous GPS stations (GSGL, GSML, QHME) position time series, before the 2016 Menyuan Ms6.4 earthquake, is it a geophysical phenomenon associated with the seismogenic process of crustal deformation, or just the presentation of some kind of non-tectonic interference? This is an interesting issue worthy of discussion. In order to answer the question, we analyze the position time series of these 3 GPS stations. Fig. 7 is the position time series of these stations after removing the linear terms in 3 components (N E U). The linear term is calculated by weighted least squares linear fit. The results show that

Table 2 – Model parameters and inverted motion rates of the major active faults around 2016 Menyuan Ms6.4 earthquake.

Name		Locked depth (km)	Dip direction	Dip angle (°)	Inverted rate	
					Slip rate (Right-lateral is positive) mm/a	Dip rate (Thrust is positive) mm/a
Qilian-Haiyuan fault system	Jinqianghe-Maomaoshan Fault	15	N	70	−8.2 ± 1.4	4.0 ± 0.8
	Lenglongling Fault	15	N	70	−4.6 ± 0.8	5.9 ± 0.8
	Tuolaishan Fault	15	N	70	−5.3 ± 0.6	6.7 ± 0.7
Xunhua-Nanshan Fault		15	N	70	−0.1 ± 0.2	2.4 ± 0.2
Riyueshan Fault		15	SW	70	2.6 ± 0.1	−1.5 ± 0.2
Huangcheng-Shuangta Fault		15	S	70	−1.0 ± 0.5	1.8 ± 0.2
Tianqiaogou-Huangyangchuan Fault		15	N	70	−2.0 ± 0.1	2.0 ± 0.2
Qilianshanbeiyuan fault system		15	S	70	−0.5 ± 0.2	3.0 ± 0.8
Longshoushan Fault		15	S	70	0.1 ± 0.1	2.6 ± 0.8

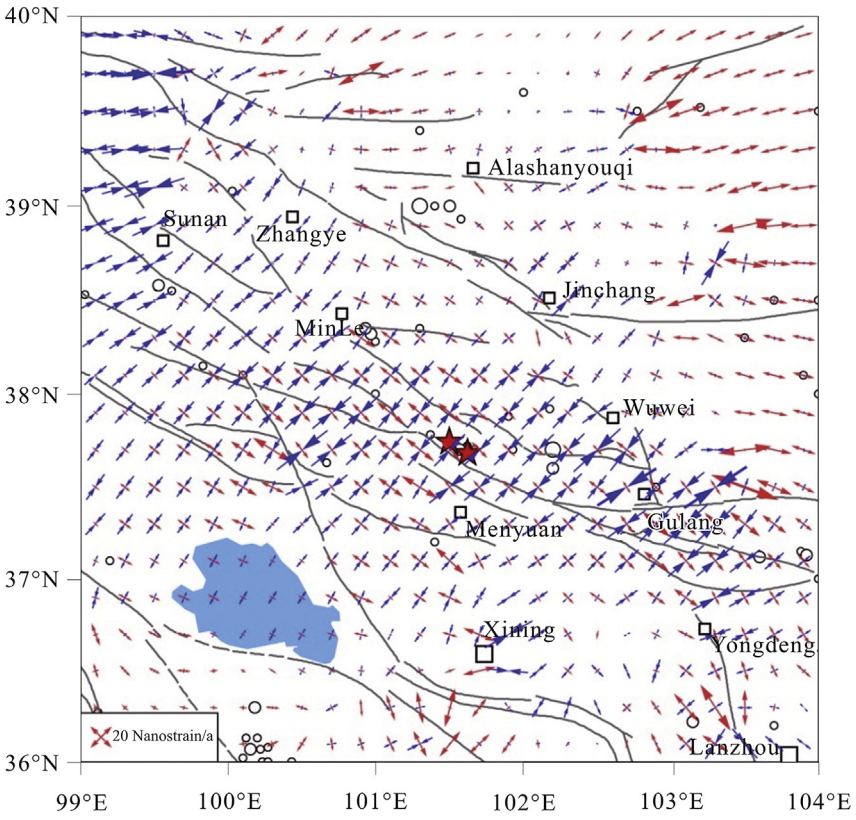

Fig. 4 – Crustal strain rate field of the region around the seismogenic area of the 2016 Menyuan Ms6.4 earthquake.

during 2010 and 2012 the time series have a remarkable dispersion, especially in the E component. The reason is that the continuous GPS stations of "CMONOC II" project were in a test run status at the period, and there were some systemic problems on the firmware of GPS equipment of all the stations. Later, the problems were found and solved in time. From Fig. 7 we can see that the position time series of all the 3 stations have been significantly improved since 2012, and show a quite good consistencies among the 3 stations, including some apparent and similar cyclical fluctuations. Recent studies show that, these consistencies of cyclical fluctuations primarily reflect the impacts of some systemic non-tectonic influence, such as seasonal variations of the loading from regional air and ground water, and the non tectonic fluctuations transferred from global reference stations of the ITRF when transforming daily solutions to ITRF [14]. But for the GPS stations which are close to each (e.g., less than 200 km), those non-tectonic influences usually have a common mode or strong time–space correlation. Therefore, the time series of dilatation and strain calculated from the position time series of these near-distance stations are not significantly affected by the non-tectonic influences. So, we believe that the non-linear or abnormal changes of the dilatation and maximum shear strain in the seismogenic region reflect some reliable tectonic phenomena of stress–strain variation before the earthquake, to a large extent. If so, what kind of physical mechanism is reflected via these tectonic phenomena obtained by GPS observations? Classical stress-strain curve of rock under uniaxial compression reveals that (Fig. 8) [15], when a rock is deformed from the linear elastic stage into the "micro rupture" phase, the linear stress–strain relationship will gradually change into a curve one. Meanwhile, the compression rate of rock volume will slow down, and the trend of horizontal strain will reverse. When the micro rupture phase goes further into the unstable rupture phase, the rock will be destructed at some weak parts at first, and then, the stress will redistribute and lead other weak parts to be destructed until all the rock to be ruptured. And the deformation of the rock is changing from compression into expansion. The non-linear or abnormal variations we observed, e.g. the dilatation of the seismogenic region is continuously reduced with a "non-linear" trend, and both the dilatation and maximum shear strain show significant inverse trends about 2–3 months before the event, coinciding well with the rock experimental results.

Jiang et al. [16–18], by analyzing the historical earthquakes ($Ms > 6$) of China, pointed out that strong earthquakes are usually distributed in the areas where the magnitude and/or direction of crustal horizontal motion have significant variations. That is, the areas with high value of shear strain or the margins of these kind of areas. The results of this study show that the epicenter of the 2016 Menyuan Ms6.4 earthquake is also located in an area with significant variation of strain, in agreement with the above conclusion.

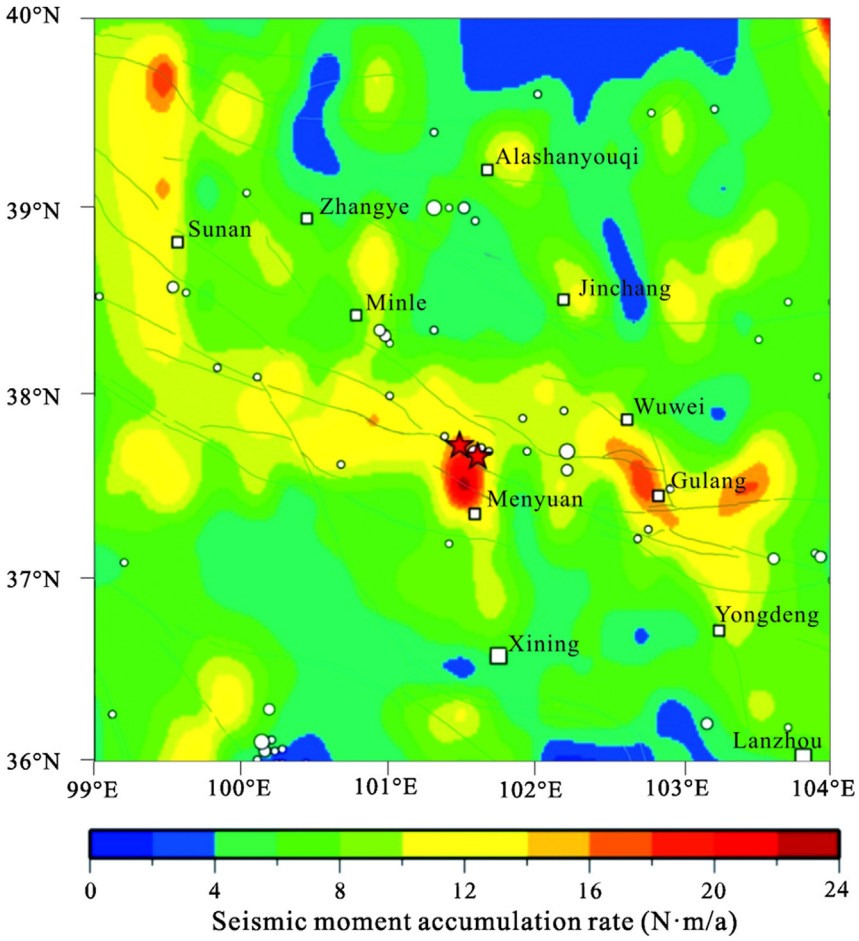

Fig. 5 – Seismic moment accumulation rate of the region around the seismogenic area of the 2016 Menyuan Ms6.4 earthquake. (20 km × 20 km grid).

Although GPS velocity field and strain rate field have made some contributions for the location prediction of strong earthquakes, we have not yet found an effective method to use them to predict the occurrence time of a strong earthquake. Some studies indicated that a sudden change in the strain (i.e. variation trend is weakened or reversed) could be a short-term precursor for earthquake prediction, and the sudden change usually occur 2–3 months before the earthquake [19,20]. The phenomena are also founded in our study, which may reflect some common mechanisms of earthquake evolution process.

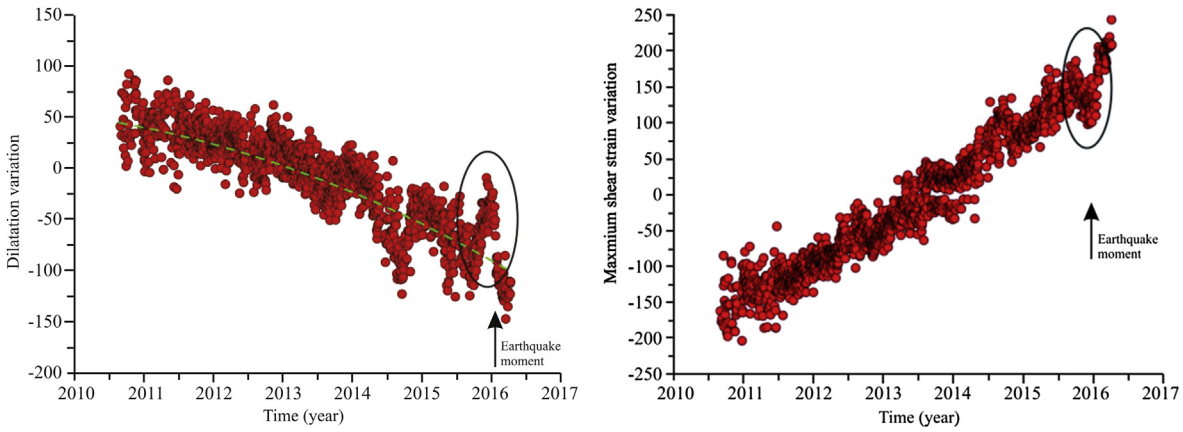

Fig. 6 – Dilatation and maximum shear strain time series of the triangle region which is formed by 3 continuous GPS stations (GSML, QHME and GSGL), and covering the seismogenic region of the 2016 Menyuan Ms6.4 earthquake.

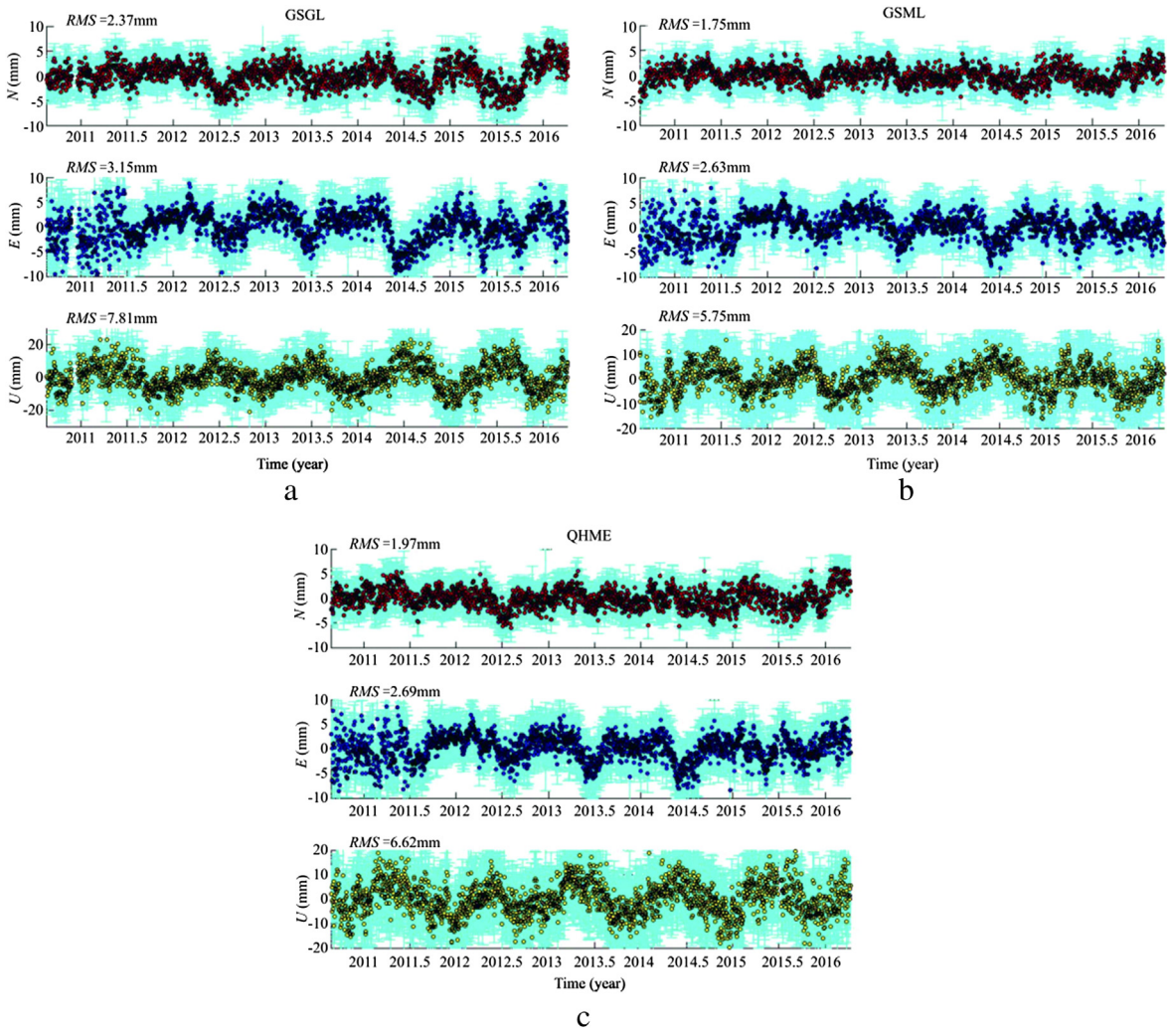

Fig. 7 – Position time series of 3 continuous GPS stations (GSGL, GSML, QHME) after removing the linear terms.

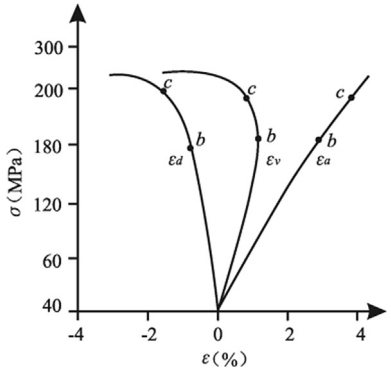

Fig. 8 – Stress–Stain relation curve of rock [15].

6. Conclusion

The 2016 Menyuan *Ms*6.4 earthquake happened at Lenglongling Fault which was belong to Qilian-Haiyuan fault system of northeastern Tibetan. Based on the velocity field from over ten years GPS observations, a regional strain rate field is calculated. The results indicate that the crustal strain rate and seismic moment accumulation rate of the Qilian-Haiyuan active fault, which is the seismogenic tectonics of the event, are significantly higher than the surrounding regions. In a 20 km × 20 km area around the seismogenic region, the maximum and minimum principal strain rates are 21.5 nanostrain/a (NW–SE extension) and −46.6 nanostrain/a (NE–SW compression), respectively, and the seismic moment accumulation rates is 17.4 Nm/a. The direction of principal compression is consistent with the focal mechanism of this event. Based on the position time series of the continuous GPS stations for a time-span of about 6 years before the event, we calculate the strain time series. The results show that the dilatation of the seismogenic region is continuously reduced with a "non-linear" trend since 2010, which means the seismogenic region has been in a state of compression. However, about 2–3 months before the event, both the dilatation and maximum shear strain show significant inverse trends. These abnormal changes of crustal deformation may reflect the nonlinear adjustment of the stress–strain accumulation of the

seismogenic region, when the accumulation is approaching the critical value of rupture.

Acknowledgments

The GPS data used in this paper are primarily from the National Key Scientific Projects "Crusta1 Movement Observation Network of China" (CMONOC I) and "Tectonic and Environmental Observation Network of Mainland China" (CMONOC II). We express our gratitude and thanks to all our Chinese participants in constructing the network and conducting the GPS measurements. This work is supported by the National Science Foundation of China (41474090), Science for Earthquake Resilience (XH14063) and the State Key Laboratory of Earthquake Dynamics (LED2013A02).

REFERENCES

[1] Yan Z, Zhang C, Xiao L. The sequence characteristics of Menyuan Earthquake on AUG 26. Northwest Seismol J 1987;9(2):89–93.
[2] Gan W, Zhang R, Zhang Y, Tang F. Development of the crustal movement observation network in China and its applications. Recent Dev World Seismol 2007;07:43–53.
[3] Gan W, Li Q, Zhang R, Shi H. Construction and application of tectonic and environmental observation network of mainland China. J Eng Stud 2012;4(04):324–31.
[4] Webb FH, Zumberge JF. An introduction to GIPSY. OASIS-II. JPL Publ; 1993D-11088.
[5] Dong D, Herring T, King R. Estimating regional deformation from a combination of space and terrestrial geodetic data. J Geod 1998;72:200–14.
[6] Böhm J, Heinkelmann R, Schuh H. Short note: a global model of pressure and temperature for geodetic applications. J Geodesy 2007;81(10):679–83.
[7] Schmid R, Steigenberger P, Gendt G, Ge M, Rothacher M. Generation of a consistent absolute phase-center correction model for GPS receiver and satellite antennas. J Geodesy 2007;81(12):781–98.
[8] Blewitt G. Fixed point theorems of GPS carrier phase ambiguity resolution and their application to massive network processing: Ambizap. J Geophys Res Solid Earth 2008;113(B12).
[9] Yuan D, Champagnac J, Ge W, Molnar P, Zhang P, Zheng W, et al. Late quaternary right-lateral slip rates of faults adjacent to the lake Qinghai, northeastern margin of the Tibetan Plateau. Geol Soc Am Bull 2011;123(9–10):2016–30.
[10] Okada Y. Internal deformation due to shear and tensile faults in a half-space. Bull Seismol Soc Am 1992;82:1018–40.
[11] Wessel P, Smith W. New, improved version of generic mapping tools released. EOS Trans Am Geophys Union 1998;79(47). 579–579.
[12] Gan W, Prescott W. Crustal deformation rates in central and eastern US inferred from GPS. Geophys Res Lett 2001;28(19):3733–6.
[13] Savage J, Svarc J. Postseismic deformation associated with the 1992 Mw=7.3 Landers earthquake, southern California. J Geophys Res Solid Earth 1997;102(B4):7565–77.
[14] Sheng C. Regional characteristics and correct model of non-tectonic loading on crustal deformation in China mainland. Institute of Geology, CEA; 2013.
[15] Shang Y. Geological engineering. Beijing: Tsinghua University Press; 2006.
[16] Jiang Z, Ma Z, Zhang X, Wang Q, Wang S. Horizontal strain field and tectonic deformation of China mainland reveled by preliminary GPS result. Chin J Geophys 2003;46(3):352–8.
[17] Jiang Z, Zhang X, Zhu Y, Zhang C, Wang S. Regional tectonic deformation setting before the Ms8.1 earthquake in the west of the Kunlun mountains pass. Sci China Ser D Earth Sci 2003;46(2):227–42.
[18] Jiang Z, Yang G, Wang M, Zhang X, Wu Y, Fang Y, et al. On crustal movement in China continent and its relationship with strong earthquakes. J Geodesy Geodyn 2006;26(3):1–9.
[19] Zhang X, Jiang Z, Wang M, Wang S, Zhao Y. On relation between crustal Movement and earthquake by use of observations of continuous GPS sites. J Geodesy Geodyn 2006;26(4):63–8.
[20] Hou H, Jiang Z. On micro-dynamic deformation informations obtained from GPS observations during KunLun mountain Ms8.1 earthquake in 2001. J Geodesy Geodyn 2008;28(3):9–13.

Weitao Chen, is an associate researcher at National Earthquake Infrastructure Service. He obtained his doctoral degree from Institute of Geology, China Earthquake Administration. His study interests include the GPS geodesy, geodynamic and seismogeodesy.